DØ Note 5931-CONF

Version 1.8

Send comments to d0-run2eb-029@fnal.gov

David Hedin, Sergey Uzunyan and $ZH \to \nu\bar{\nu}b\bar{b}$ team[1]

Search for Third Generation Leptoquarks and Scalar Bottom Quarks in the $b\bar{b}$ plus Missing Energy Topology in $p\bar{p}$ collisions at $\sqrt{s} = 1.96$ TeV

(Dated: June 30, 2009)

We study a final state with missing energy and two b quarks using 4.0 fb^{-1} of DØ Run II data. Such a state could result from either third generation leptoquark pair production or from scalar bottom quark pair production. We present preliminary results on an analysis where both leptoquarks are assumed to decay into neutrinos plus b quarks or both bottom squarks decay into neutralinos plus b quarks, with the neutralino assumed to be the lightest supersymmetric particle. We exclude at the 95% confidence level third generation scalar leptoquarks with $M_{LQ} < 252$ GeV/c^2, and set 95% C.L. limits in the $(m_{\tilde{b}_1}, m_{\tilde{\chi}_1^0})$ mass plane, improving previous Tevatron results.

Preliminary Results for Summer 2009 Conferences

[1] Samuel Calvet, Theo Christoudias, Tyler Dorland, Abhinav Dubey, Gabriel Facini, Jean-Francois Grivaz, Gavin Hesketh, Remigius K Mommsen, Christophe Ochando, Krisztian Peters, Murilo Range

I. INTRODUCTION

Leptoquarks (LQ) are exotic particles that have color, electric charge, and both lepton and baryon numbers and appear in extended gauge theories and composite models. Current theory suggests that leptoquarks would come in three different generations corresponding to the three quark and lepton generations. Charge 1/3 third generation leptoquarks would decay into either a tau neutrino plus a b quark or, if heavy enough, to a tau lepton plus a t quark. Leptoquarks can be either scalar or vector particles. This analysis sets limits for scalar leptoquarks for which the cross section is lower and computed to higher order in perturbation theory.

A different extension of the Standard Model (SM), supersymmetry, assigns a bosonic superpartner to every SM fermion and vice-versa. The supersymmetric quarks (squarks) are mixtures of the superpartners $\tilde{q}_L$ and $\tilde{q}_R$ of the SM quark helicity states q_L and q_R. The theory permits a mass difference between squark mass eigenstates, $\tilde{q}_1$ and $\tilde{q}_2$ that gives the possibility that the lightest states of the stop and sbottom quarks are lighter than the first two generation squarks. In this analysis we consider the region of SUSY parameter space where the only possible decay of the sbottom quark's lightest state is $\tilde{b}_1 \to b\tilde{\chi}_1^0$, $m_{\tilde{b}_1} > m_b + m_{\tilde{\chi}_1^0}$ and $m_{\tilde{b}_1} < m_t + m_{\tilde{\chi}_1^\pm}$, where the neutralino $\tilde{\chi}_1^0$ and chargino $\tilde{\chi}_1^\pm$ are the lightest SUSY partners of the electroweak bosons. In the minimal supersymmetric standard model (MSSM) [1] the $\tilde{\chi}_1^0$ is stable and all SUSY particles are pair produced, and we therefore search for $p\bar{p} \to \tilde{b}_1\bar{\tilde{b}}_1 \to b\tilde{\chi}_1^0\bar{b}\tilde{\chi}_1^0$.

At the Tevatron, leptoquarks or sbottom pairs would be produced mainly through $q\bar{q}$ annihilation or gg fusion with identical leading order production cross sections. For limit setting we used the next-to-leading order (NLO) cross sections [2] for the leptoquark production, while the NLO cross sections for the sbottom pair production were calculated with PROSPINO-2 [3].

The detector signature of the final state are two acoplanar b-jets from the leptoquarks or the scalar bottom quarks and the missing energy due to escaping neutrinos or neutralinos. The current limit on the LQ_3 mass in this channel established by DØ based on the Fermilab Run IIa data is 229 GeV [4]. For direct production of sbottom quarks the mass is restricted to be larger than 222 GeV for the massless neutralino in the DØ analysis [5] and to 193 GeV for $m_{\tilde{\chi}_1^0} = 40$ GeV in the CDF Run II (295 pb^{-1}) search [6]. The previous DØ results used a 310 pb^{-1} sample triggered by missing transverse energy, missing transverse energy, and, for the leptoquark search only, an additional muon+jet trigger sample of 425 pb^{-1}.

II. DATA SAMPLES

This note describes the analysis of the Run II DØ data set collected through December 2008. Data was collected by the DØ detector [7] using different jet plus missing energy triggers during different time periods. At the start of the DØ Run II, the trigger required at least three calorimeter trigger towers with $E_T > 5$ GeV at Level 1 and the vector sum of the jets' transverse energy, defined as $\not\!\!H_T \equiv |\sum_{jets} \vec{p_T}|$, was required to be > 20 GeV at Level 2 and > 30 GeV at Level 3. Later it was modified by also requiring that the acoplanarity, defined as the azimuthal angle between the two leading jets, be $< 169°$, and the scalar sum of jet p_T, H_T, be > 50 GeV. A total of 945 pb^{-1} was collected with these triggers. In 2006 the improved DØ trigger system allowed the $\not\!\!H_T$ requirement to be lowered to 25 GeV and the $\not\!\!E_T$ to be used at Level 1. The total data sample, after imposing the DØ quality requirements, corresponds to an effective integrated luminosity of 3.98 ± 0.24 fb^{-1}.

III. DEFINITION OF OBJECTS

Electromagnetic (EM) objects are identified using the pattern of energy deposited in the calorimeter while muons are required to have hits in both the muon wire chambers and scintillation counters. Jets are reconstructed by a cone algorithm with radius $\Delta R = \sqrt{(\Delta\eta)^2 + (\Delta\phi)^2} = 0.5$ in pseudorapidity (η) and azimuthal angle (ϕ) space about the jet's axis. Good jets correspond to the criteria: (a) $0.05 <$ electromagnetic fraction of the energy < 0.95; (b) the fraction of energy in the outermost part of the calorimeter < 0.4; (c) confirmed by the Level 1 trigger; and (d) there are no reconstructed EM objects with p_T over 5 GeV in $\Delta R_{EM-jet} < 0.4$. The missing transverse energy, $\not\!\!E_T$, is determined by the vector sum of the transverse components of the energy deposited in the calorimeter and the p_T of detected muons. We used all good jets in the event to calculate $\not\!\!H_T$ and H_T, the scalar sum of the p_T of these jets. To discriminate events with real $\not\!\!E_T$ from the events from fake or mismeasured $\not\!\!E_T$ we used two additional parameters: the missing transverse energy significance, denoted as $msig$, to estimate how consistent the observed $\not\!\!E_T$ is with respect to what can be expected from jet energy measurement fluctuations, and the ($\not\!\!E_T$,$\not\!\!H_T$) asymmetry $A \equiv (\not\!\!E_T - \not\!\!H_T)/(\not\!\!E_T + \not\!\!H_T)$.

IV. SIGNAL AND BACKGROUND SAMPLES

The signal MC samples for scalar leptoquark masses 200–280 GeV and the $(\tilde{b}_1, \tilde{\chi}_1^0)$ pairs with sbottom and neutralino masses of 80–260 GeV and 0–100 GeV were generated with PYTHIA 6.323 [9]. Physical backgrounds include processes with real $\not\!\!E_T$. We label these as SM processes and background from them was estimated using MC events. The most important are leptonic decays of W/Z bosons + jets such as $Z \to \nu\bar{\nu}$ or $W \to e\nu$ when the leptons remain unreconstructed or are misidentified as hadrons, and processes with a t quark. For all SM samples the cross sections used to estimate their contribution to the background were obtained from Refs. [10] and [11]. At the parton level the single top MC was generated with COMPHEP 4.4 [12] and ALPGEN [13] was used for all other samples. All MC events were then processed with PYTHIA, which performed showering and hadronization. To model the events of multiple interactions and detector noise, data events from random $p\bar{p}$ crossings are overlaid on SM MC events. The resulting samples were processed using a full GEANT [14] simulation of the DØ detector. CTEQ6L1 [15] were used as parton density functions in all cases.

Instrumental background to our signal comes mostly from multijet processes with $\not\!\!E_T$ arising from mismeasurement. This background, which we label QCD, dominates the low $\not\!\!E_T$ region, and was modeled from data.

V. EVENT SELECTION

A. The signal sample

We selected events with exactly two or three jets with $|\eta_{det}| < 2.4$ and $E_T > 20$ GeV, where η_{det} is the pseudorapidity defined using the the detector center as the origin. We also required that the primary vertex have at least three tracks and be within ± 40 cm in the beam direction from the center of the detector, and that $\not\!\!E_T > 20$ GeV. As the leading jets in our signals are assumed to originate from the decay of b quarks we required the first two leading jets in the selected events to have at least two tracks pointing to the event primary vertex. To help reduce the contribution from $W \to l\nu$ decays, we vetoed events with isolated EM objects or isolated muons with $p_T > 15$ GeV. We required the leptons to be separated from jets by $\Delta R_{l-jet} > 0.5$, also required the leading jets acoplanarity $< 165^\circ$. To suppress the instrumental background we required the $\not\!\!E_T > 40$ GeV and removed those events where the $\not\!\!E_T$ direction overlapped a jet in ϕ by appling the "triangle" cut: $\not\!\!E_T/\text{GeV} > 80 - 40 \times \Delta\phi_{min}(\not\!\!E_T, jets)$, where $\Delta\phi_{min}(\not\!\!E_T, jets)$ denotes the minimum angle between $\not\!\!E_T$ and any of the selected jets and is measured in radians. We vetoed events which contained any jet that failed the good jet criteria and had $E_T > 15$ GeV. For a large fraction of events with a mismeasured $\not\!\!E_T$, the direction of $\not\!\!E_T$ is not aligned with the missing track $\not\!p_T$, calculated as the negative of the vectorial sum of charged particles transverse momenta, and we required $\Delta\phi(\not\!\!E_T, \not\!p_T) < \pi/2$. Table I shows the number of data events and acceptances for the signals (accounting for the trigger efficiency parameterization) after different selections.

TABLE I: Number of data events and expected signal acceptance after different cuts.

Selection	Data, events	M_{LQ}=220 [GeV] accept., %	$(m_{\tilde{b}_1}, m_{\tilde{\chi}_1^0})$=(240,0) [GeV] accept., %	$(m_{\tilde{b}_1}, m_{\tilde{\chi}_1^0})$=(100,60) [GeV] accept., %
trigger, Njet=2,3	15928418	59.0	61.3	11.2
$\lvert PV_Z\rvert < 40$ cm, $PV_{ntrk} > 2$	13778458	53.6	55.9	10.2
$\not\!\!E_T > 20$ GeV	10228729	53.6	55.8	10.2
Taggable jet_1 and jet_2	9037473	50.8	52.7	9.7
no isolated leptons p_T >15 GeV	8995401	50.8	52.7	9.7
acoplanarity $< 165^\circ$	7059765	48.7	50.6	9.3
$\not\!\!E_T > 40$ GeV and triangle cut	435099	43.8	45.6	7.7
bad jets veto	363899	43.8	45.5	7.7
$\Delta\phi(\not\!\!E_T, \not\!p_T) < \pi/2$	221131	42.3	44.2	7.4

B. W-control sample and QCD background estimation

We used two additional data samples to improve the accuracy of our description of the SM backgrounds and to model the multijet background contribution. First we selected a W sample that was almost free from multijet background and should be described accurately by the MC simulation. We used similar initial selections as for the signal sample, but only required that $\not\!\!E_T > 30$ GeV. We inverted the isolated lepton veto and required the presence

of an isolated muon with $p_T^\mu > 15$ GeV with $|\eta| < 2$. To obtain a clean W sample we required the W transverse mass be greater then 30 GeV, vetoed events with bad jets, and required $-0.1 < A(\not\!\!E_T, \not\!\!H_T) < 0.2$. After these selections $V + jets$ MC was normalized to the number of events in data, and we used the scale factor obtained in all subsequent selections. Figure 1 gives the W transverse mass and the $\not\!\!E_T$ distributions for this sample.

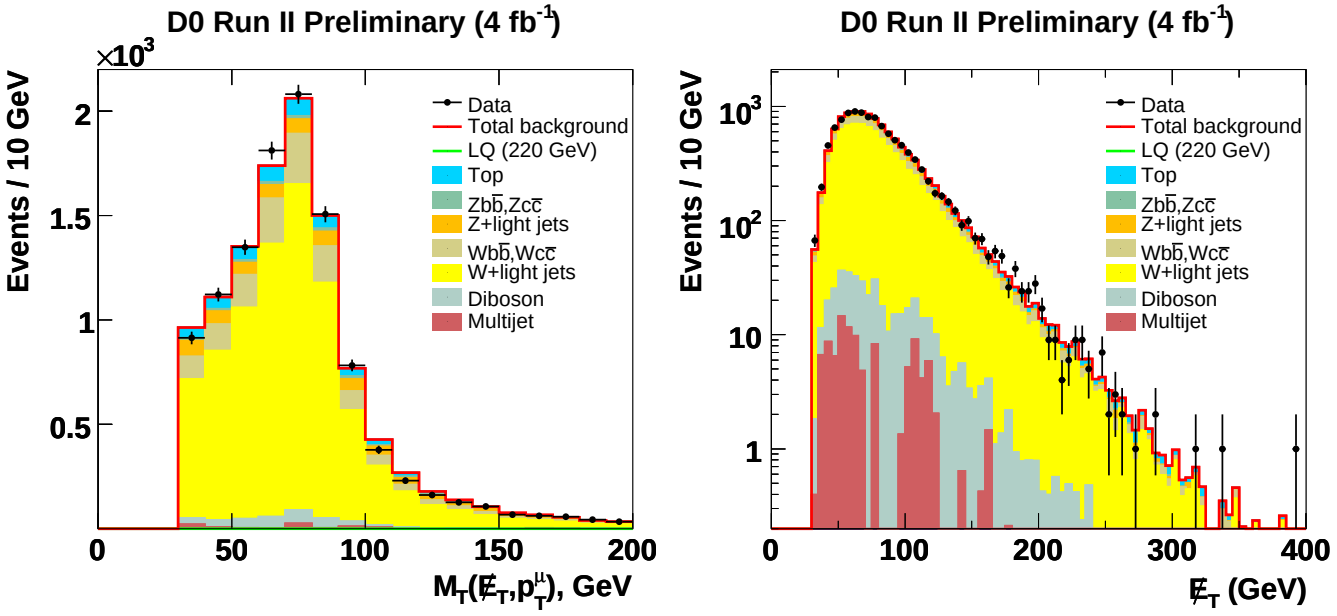

(a) (b)

FIG. 1: (a) The W transverse mass and (b) the $\not\!\!E_T$ distributions for the W-control sample. The points are data while the color histograms show the individual contribution of the SM processes.

We define a second auxiliary sample to model the QCD multijet process. Here we exploit the difference between the directions of MET and MpT. For well measured events these directions should be similar, whereas for mismeasured multijet events they can differ substantially [16]. We therefore selected events with $\Delta\phi(\not\!\!E_T, \not\!p_T) > \pi/2$ to model the kinematic distributions of the QCD multijet background after subtracting the small contribution from SM processes to those events and removing events that have a poor $\not\!p_T$ measurement due to missing tracks in the leading jet. The scale factor for the QCD background was obtained by requiring the number of data events be equal to the sum of SM and QCD in the $\Delta\phi(\not\!\!E_T, \not\!p_T) < \pi/2$ region. This scale factor was used with the kinematic distributions of the events with $\Delta\phi(\not\!\!E_T, \not\!p_T) > \pi/2$ to obtain the QCD distributions for other kinematic quantities.

For the signal sample, events with poorly measured $\not\!\!E_T$ were reduced by requiring that $-0.1 < A(\not\!\!E_T, \not\!\!H_T) < 0.2$, $\not\!\!E_T$ significance $msig > 5$, and $\Delta\phi_{min}(\not\!\!E_T, jets) > 0.6$ rad. Figure 2 shows distributions of $\not\!\!E_T$ and the the scalar H_T after these selections with the LQ and SM events normalized to the integrated luminosity and the QCD background modelled as described above.

C. b-tagging and final selections

The neural network (NN) b-tagging tool [17] combines the algorithms that use DØ tracker information to identify the heavy-flavor jets while significantly reducing the SM and QCD backgrounds which are dominated by light flavor jets. The algorithm provides the possibility to varying the requirements on its output to maximize the sensitivity to the LQ_3 and sbottom signals. We applied the NN b-tagging to the one or two leading jets in our signal, data, and background samples and choose the requirements on the NN-output to have one jet tagged with an efficiency of 70% and the other with an efficiency of 45%, where the corresponding probabilities of a b-jet to be wrongly identified as a light flavor jets are 5% and 0.5%. These conditions correspond to the maximum expected mass limits after all other cuts were applied. The $\not\!\!E_T$ and H_T distributions after b-tagging and cuts on $\not\!\!E_T$ quality are shown in Fig. 3 with a $M_{LQ_3} = 220$ GeV signal. We then applied additional selections to futher improve the sensitivity to our signals. As our signals consist of two high E_T b-jets, we used the $X_{jj} \equiv (E_T^{jet1} + E_T^{jet2})/(\Sigma_{jets} E_T)$ variable as a discriminant against top quark processes, requiring $X_{jj} > 0.9$. Finally we optimized the cuts on E_T^{jet1}, $\not\!\!E_T$ and H_T for the different LQ_3

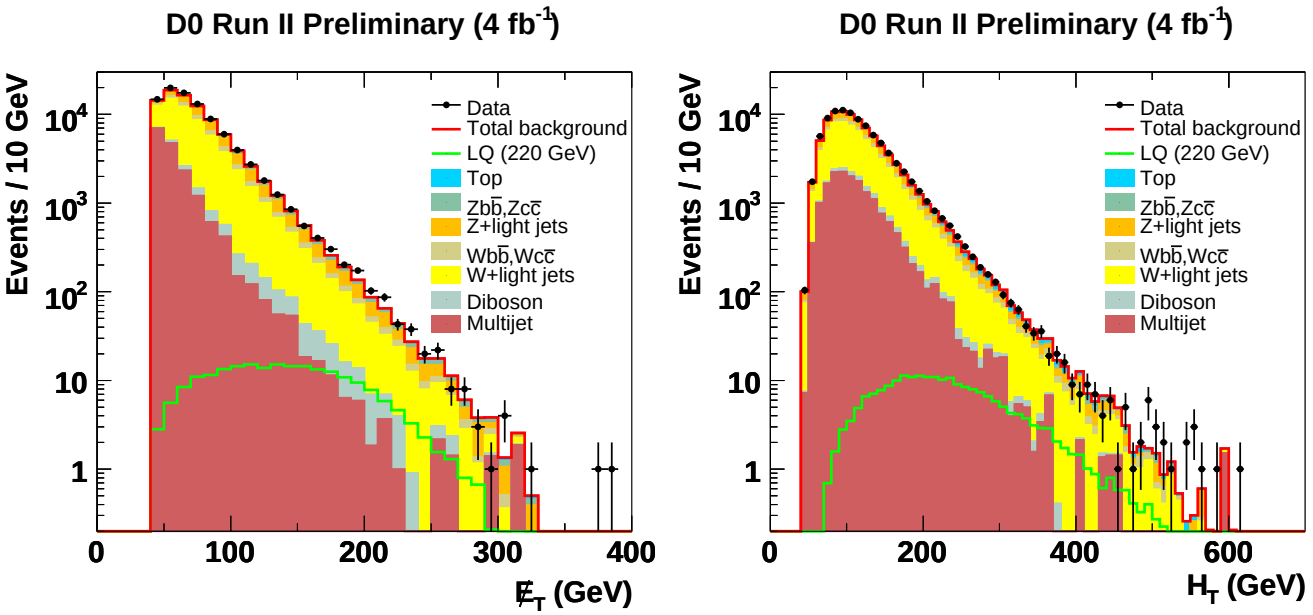

(a) (b)

FIG. 2: Signal sample. (a) The $\not\!\!E_T$ and (b) the scalar H_T after the cuts on $\not\!\!E_T$ quality (see text) and before b-tagging. The points are data while the color histograms show the individual contribution of the SM processes.

and $(m_{\tilde{b}_1}, m_{\tilde{\chi}_1^0})$ signals. These selections are tighter for the high-mass LQ_3 and sbottom signals with large $\not\!\!E_T$. For the regions with a low $m_{\tilde{b}_1} - m_{\tilde{\chi}_1^0}$, the $\not\!\!E_T$ and jet energies are lower and we used relaxed thresholds. Figure 4 shows the distributions of X_{jj} and E_T^{jet1} after the b-tagging requirements but before these final kinematic requirements.

VI. SYSTEMATIC UNCERTAINTIES

Sources of systematic uncertainties included errors on the determination of the integrated luminosity and SM cross sections, trigger parameterization, jet reconstruction efficiencies (JRE), jet energy resolution (JER), and jet energy scale (JES) corrections. Uncertainties associated with the applied b-tag algorithm include errors on the b-tag efficiency corrections for the MC jets, and errors on the selection of taggable jets that came from the vertex confirmation requirement and the uncertainty on the jet taggability efficiency. For all sources we used an estimation based on the results of $HZ \to b\bar{b}\nu\bar{\nu}$ analysis of the same signal topology [16]. Systematic uncertainties are summarized in Table II.

TABLE II: Systematic Uncertainty Summary; values given in percent.

Integrated luminosity	SM cross sections	Trigger efficiency	JES	JER	JRE	Jet selection	b-tagging efficiency
±6.1	±10	±5	±3.0	±1.0	±7.0	±5.4	±7.0

VII. RESULTS

The results of the event selection and the predicted number of events from SM and QCD multijet processes are listed in Table III. Two different selections to optimize the large and small MET sbottom searches are shown. The largest contributions come from $W/Z + b\bar{b}$ production and top quark backgrounds for the high-$\not\!\!E_T$ signals. The sbottom signal selections with a low $\not\!\!E_T$ also have a large contribution from QCD sources. We obtained the $\sigma \times B^2$ limits, where B is the branching fraction into the b quark plus neutrino channel for LQ decays or into the b plus

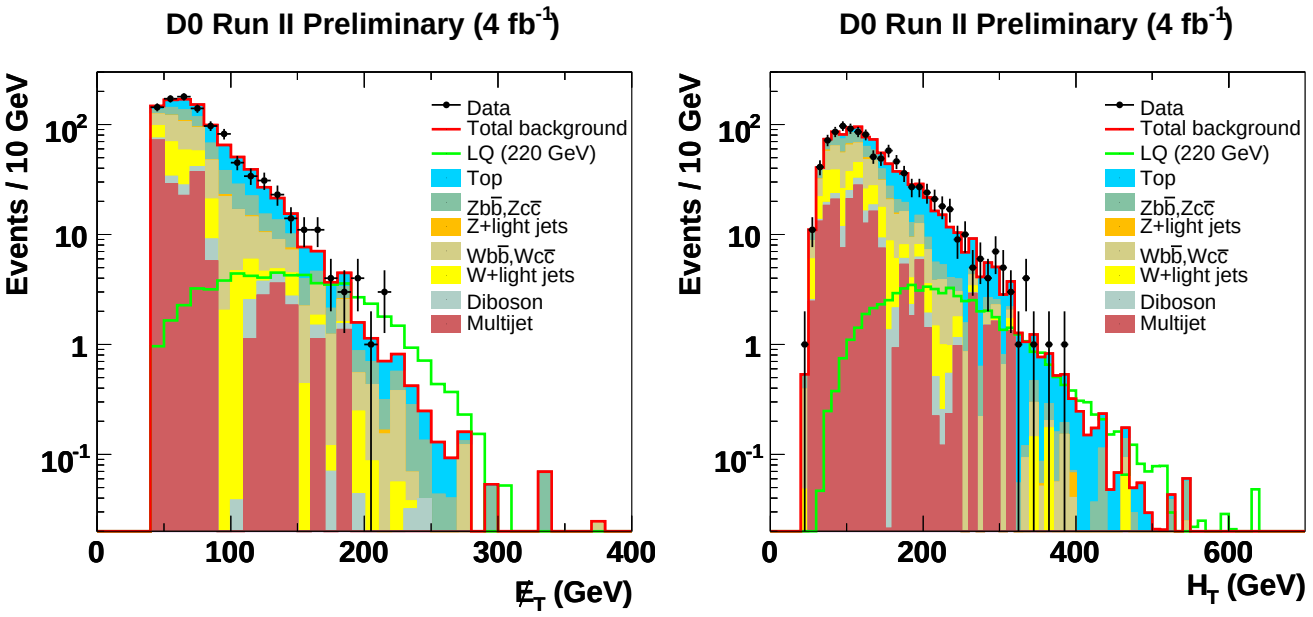

(a) (b)

FIG. 3: (a) The $\not\!\!E_T$ and (b) the scalar H_T after b-tagging and the cuts on $\not\!\!E_T$ quality. The points are data while the color histograms show the individual contribution of the background processes.

LSP for sbottom decays, using the CL_s approach [18]. In this technique, an ensemble of MC experiments using data, signal and background events fluctuated within their uncertainties are used to derive an exclusion, taking into account the correlations among the systematic uncertainties on the signal and backgrounds. The final LQ results are given in Table IV. For higher mass points, three events remain in the data compared to an expected $3.2 \pm 0.3 \pm 0.6$ events from background processes. Figure 5(a) shows the 95% C.L. cross section limits as a function of M_{LQ}. Limits on the LQ_3 mass were obtained by the intersection of the observed cross section limit (solid line) with the center line of theory, giving a limit of 252 GeV for $B = 1$. If we account for the variation of the factorization/renormalization scale by a factor of two about $\mu = M_{LQ}$ and include the PDF errors, then the 95% C.L. cross section limit on leptoquark mass achieved at the intersection with the lower edge of the theory band is 245 GeV for $B = 1$. Also shown is the central theory band when the coupling of a charge 1/3 LQ to the νb and τt channels are identical yielding $B = 1 - 0.5 \times F_{sp}$ where F_{sp} is a phase space suppression factor for the τt channel. The cross section limit in this case is 239 GeV.

Figure 5(b) shows the 95% C.L. and excluded region in the sbottom mass versus neutralino mass plane. For $m_{\tilde{\chi}_1^0} = 0$, the limit is $m_{\tilde{b}_1} > 255$ GeV. The exclusion region extends up $m_{\tilde{\chi}_1^0} = 90$ GeV for $m_{\tilde{b}_1}$ in the range 150–200 GeV.

VIII. SUMMARY

A 4 fb^{-1} data sample collected with acoplanar jets plus missing transverse energy triggers were analyzed using a neural-net b-tagging algorithm. After requirements on $\not\!\!E_T$ and double b-tagging, the number of events which passed our selection cuts agreed with the expectations from known processes. Assuming a decay into the $\nu\bar{\nu}b\bar{b}$ channel with $B(LQ \to \nu b) = 1$, a mass limit of 252 GeV for charge 1/3 third generation leptoquarks was obtained. We also exclude the production of scalar bottom quarks for a range of values in the $(m_{\tilde{b}_1}, m_{\tilde{\chi}_1^0})$ mass plane. These limits improve on previously available results.

Acknowledgments

We thank the staffs at Fermilab and collaborating institutions, and acknowledge support from the DOE and NSF (USA); CEA and CNRS/IN2P3 (France); FASI, Rosatom and RFBR (Russia); CNPq, FAPERJ, FAPESP and

TABLE III: Predicted number of events and the signal acceptance (in parentheses) before and after b-tagging and additional event selections (statistical errors only).

Process	Pretag	b-tag	$msig > 5$, $-0.1 < A < 0.2$, $\Delta\phi(\not\!\!E_T, jets) > 0.6$ rad	$X_{jj} > 0.9$ $E_T^{jet1} > 20$ [GeV] $\not\!\!E_T > 40$ [GeV] $H_T > 60$ [GeV]	$X_{jj} > 0.9$ $E_T^{jet1} > 50$ [GeV] $\not\!\!E_T > 130$ [GeV] $H_T > 230$ [GeV]
Diboson	1951 ± 8	33 ± 1	30 ± 1	17 ± 1	0.3 ± 0.1
$W(\to l\nu)$+ light jets	52604 ± 87	154 ± 7	133 ± 7	85 ± 6	0.3 ± 0.1
$Wc\bar{c}, Wb\bar{b}$	6577 ± 24	275 ± 4	245 ± 4	128 ± 3	1.7 ± 0.3
$Z(\to ll)$ + light jets	14457 ± 67	10 ± 2	8 ± 2	7 ± 2	0
$Zc\bar{c}, Zb\bar{b}$	3274 ± 19	165 ± 3	155 ± 3	109 ± 2	2.2 ± 0.3
Top	1703 ± 3	285 ± 1	240 ± 1	73 ± 0	2.9 ± 0.1
Multijet	140565 ± 384	776 ± 29	169 ± 15	73 ± 10	0
Total background	221131	1699 ± 31	981 ± 17	493 ± 12	7.1 ± 0.4
# data events	221131	1814	998	483	7
Signal (acceptance, %)					
$M_{LQ} = 220$ GeV	237 ± 2 (42.3)	68 ± 1 (12.0)	63 ± 1 (11.2)	—-	17.0 ± 0.5 (3.0)
$(m_{\tilde{b}_1}, m_{\tilde{\chi}_1^0})$=(240,0) GeV	139 ± 1 (44.2)	40 ± 1 (12.7)	36 ± 1 (11.5)	– – – –	11.4 ± 0.2 (3.6)
$(m_{\tilde{b}_1}, m_{\tilde{\chi}_1^0})$=(100,60) GeV	4416 ± 95 (7.4)	996 ± 39 (1.7)	906 ± 37 (1.5)	610 ± 29 (1.0)	—-

FUNDUNESP (Brazil); DAE and DST (India); Colciencias (Colombia); CONACyT (Mexico); KRF and KOSEF (Korea); CONICET and UBACyT (Argentina); FOM (The Netherlands); STFC and the Royal Society (United Kingdom); MSMT and GACR (Czech Republic); CRC Program, CFI, NSERC and WestGrid Project (Canada); BMBF and DFG (Germany); SFI (Ireland); The Swedish Research Council (Sweden); CAS and CNSF (China); and the Alexander von Humboldt Foundation (Germany).

[1] P. Fayet, Phys. Rev. Lett. **69**, 489 (1977).

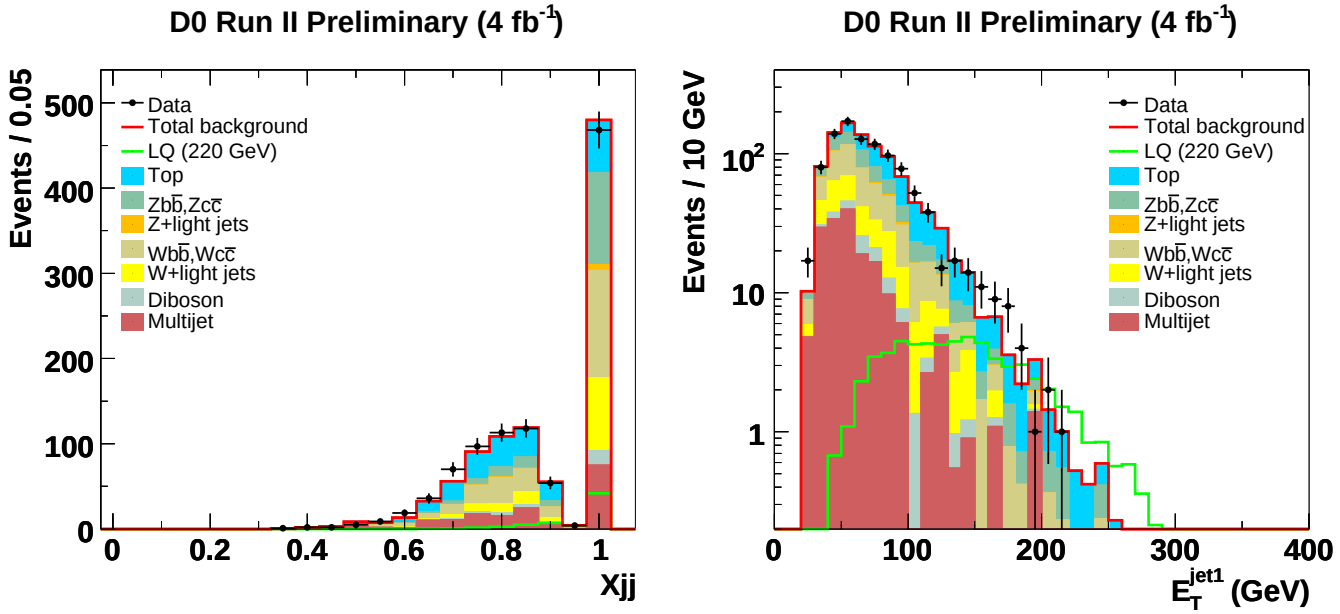

(a) (b)

FIG. 4: (a) the X_{jj} parameter, (b) the leading jet E_T after b-tagging and the cuts on $\not\!\!E_T$ quality. The points are data, color histograms show the individual contribution of the background processes.

TABLE IV: The number of observed and expected events, the signal acceptance (in parentheses), and the observed and expected 95% C.L. limits for different M_{LQ} for an integrated luminosity of 4 fb^{-1}.

M_{LQ} (GeV)	($\not\!\!E_T, H_T$) (GeV)	Data	(SM+QCD)±stat±sys	Signal (acpt,%)	95% CL, pb obs/exp
200	(130,220)	7	7.1±0.5±1.2	23.2±0.8±3.3 (2.1)	0.097/0.097
220	(130,220)	7	7.1±0.5±1.2	17.0±0.5±2.4 (3.0)	0.069/0.069
240	(130,220)	7	7.1±0.5±1.2	10.9±0.3±1.5 (3.6)	0.058/0.058
260	(150,240)	3	3.2±0.3±0.6	5.0±0.1±0.7 (3.0)	0.049/0.049
280	(150,240)	3	3.2±0.3±0.6	3.9±0.1±0.5 (3.4)	0.043/0.043

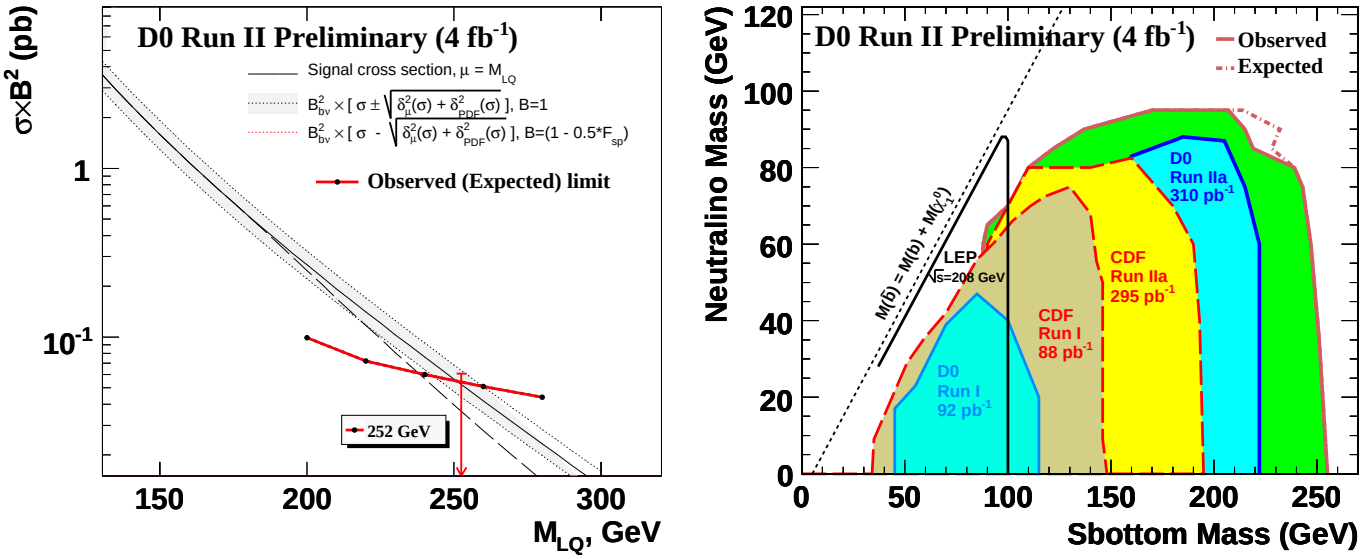

(a) (b)

FIG. 5: a) The 95% C.L. limit on $\sigma \times B^2_{b\nu}$ (points plus solid line) as a function of M_{LQ} for the pair production of third generation leptoquarks. The theory band is shown in grey with an error range as discussed in the text. The long-dashed line indicates the threshold effect for the τt channel. The expected cross section limits are same as the observed. b) The 95% C.L. exclusion contour in $(m_{\tilde{b}_1}, m_{\tilde{\chi}^0_1})$ mass plane. Also presented results from previous searches at LEP and at the Tevatron.

[2] M. Kramer, T. Plehn, M. Spira and P. M. Zerwas, Phys. Rev. Lett. **79**, 341 (1997).
[3] W. Beenaakker *et al.*, Nukl.Phys. B 515, 3 (1998)
[4] D0 Collaboration, V. Abazov *et al.*, Phys. Rev. Lett. **99**, 061801 (2007).
[5] D0 Collaboration, V. Abazov *et al.*, Phys. Rev. Lett. **97**, 171806 (2006).
[6] CDF Collaboration, T. Aaltonen *et al.*, Phys. Rev. Lett. **76**, 072010 (2007).
[7] D0 Collaboration, V. Abazov *et al.*, Nucl. Instrum. Methods A **565**, 463 (2006).
[8] CDF Collaboration, F. Abe *et al.*, Phys. Rev. Lett. **78**, 2906 (1997).
[9] T. Sjostrand *et al.*, Computer Phys. Commun. 135 238 (2001).
[10] J.M. Campbell and R.K. Ellis , Phys.Rev. D **60**, 113006 (1999); J.M. Campbell and R.K. Ellis , Phys.Rev. D **62**, 114012 (2000).
[11] M. Cacciari *et al.*, JHEP **404**, 068 (2004); N. Kidonakis and R. Vogt, Phys. Rev. Lett. D **68**, 114014 (2003); N. Kidonakis, Phys. Rev. D **74**, 114012 (2006).
[12] E. Boos *et al.*, [CompHEP Collaboration], Nucl. Instrum. Methods A **534**, 250 (2004).
[13] M.L Mangano *et al.*, JHEP **0307**,001 (2003).
[14] A. Agostinelli *et al.*, Nucl. Instrum. Methods A **506**,250 (2003).
[15] J. Pumplin *et al.*, JHEP **0207**, 012 (2002); D. Stump *et al.*, JHEP **0310**, 046 (2003).
[16] D0 Collaboration, V. Abazov *et al.*, D0 Note 5586-CONF (2008).
[17] T. Scanlon, FERMILAB-THESIS-2006-43.
[18] T. Junk, Nucl. Instrum. Methods A **434**, 435 (1999).